Phys. Status Solidi B **252,** No. 2, 391–396 (2015) / **DOI** 10.1002/pssb.201451340

physica status solidi b
www.pss-b.com
basic solid state physics

Photoemission investigation of the Schottky barrier at the Sc/3C-SiC (111) interface

Sean W. King[*,1,#], **Robert J. Nemanich**[2,##], **and Robert F. Davis**[1,###]

[1] Department of Materials Science and Engineering, North Carolina State University, Raleigh, NC 27695, USA
[2] Department of Physics, North Carolina State University, Raleigh, NC 27695, USA

Received 7 July 2014, revised 13 September 2014, accepted 22 September 2014

Keywords scandium, silicon carbide, Schottky barrier, XPS

---

[*] Corresponding author: e-mail sean.king@intel.com, Phone: +1 503 613 7547, Fax: +1 503 613 8964
[#] Presently at: Logic Technology Development, Intel Corporation, Hillsboro, OR 97124, USA.
[##] Presently at: Department of Physics, Arizona State University, Tempe, AZ 85287, USA.
[###] Presently at: Department of Materials Science and Engineering, Carnegie Mellon University, Pittsburgh, PA 15123, USA.

The Schottky barrier and interfacial chemistry for interfaces formed by evaporation of Sc onto 3C-SiC (111)-(1x1) surfaces at 600 °C has been investigated using *in situ* X-ray and ultraviolet photoelectron spectroscopy (XPS and UPS) and low energy electron diffraction (LEED). Sc was observed to grow in a two-dimensional manner and exhibit a (1x1) LEED pattern up to thicknesses of ~2 nm beyond which diffraction patterns were no longer observable. XPS measurements of these same films showed a clear reaction of Sc with the 3C-SiC (111)-(1x1) surface to form a $ScSi_x$ and ScC_x interfacial layer in addition to the formation of a metallic Sc film. XPS measurements also showed the deposition of Sc induced ~0.5 eV of upward band bending resulting in a Schottky barrier of 0.65 ± 0.15 eV.

1 Introduction

Scandium (Sc) is a rare-earth transition metal that crystallizes in the hexagonal close packed structure ($a_0 = 0.3309$ nm) and has a relatively high melting point of 2087 °C [1]. Sc is most commonly utilized as an alloying agent to minimize grain growth in aluminum alloys for a variety of athletic and aeronautical applications [2]. More recently, Sc has garnered significant interest as an electrical contact metal [1], conductive dislocation reducing buffer layer [3, 4], and alloying agent with aluminum nitride (AlN) and gallium nitride (GaN) for a variety of piezoelectronic [5–7], thermoelectric [8], ferroelectric [9], and optoelectronic applications [10–12]. This interest is primarily a result of the high solubility and close lattice matching of Sc with wurtzite structure AlN and GaN ($a_0 = 0.3111$ and 0.3189 nm), high thermal stability, ductility, and relative ease of deposition [1]. Sc also exhibits reasonably close lattice matching to the (111)/(0001) basal plane of cubic and hexagonal silicon carbide (SiC, $a_0 = 0.308$ nm). Therefore, Sc could also serve as a potential Ohmic or Schottky contact for high temperature, power, and frequency SiC based electronic devices and as a conductive buffer layer for GaN heteroepitaxy on SiC substrates. For these specific applications, the band alignment of Sc to SiC will play a significant role in charge transport and carrier recombination at these interfaces. However, Sc/SiC interfaces have gone relatively unexplored [13]. In this regard, we have utilized *in-situ* X-ray and UV photoelectron spectroscopy (XPS and UPS) to investigate the chemical structure and Schottky barrier formed at interfaces prepared by thermal evaporation of Sc directly onto 3C–SiC/6H-SiC (0001) substrates.

2 Experimental procedure

The Sc evaporation was performed in a custom built system specifically designed for the gas source molecular beam epitaxy (GSMBE) of ScN, GaN, and AlN on SiC substrates. The details of this system have been previously described [14–16]. Due to a relatively high vapor pressure, Sc was successfully evaporated/sublimed onto the SiC substrate using a Knudsen cell operated at a temperature of 1230 °C [14]. Typical impurities in scandium (Al, Ca, Cr, Cu, Mn, Si, and Y) were each ≤30 parts per million according to the manufacturer (Alfa-Aesar) and not detected during *in-situ* AES and XPS measurements of test Sc films evaporated onto Si (100) and 6H-SiC (0001) substrates. However, as will be shown later, significant amounts of fluorine (<5 at%) were detected by XPS and attributed to the scandium charge [14, 17]. The deposition rate and thickness of the Sc layers was estimated using the calculated vapor pressure of Sc and assuming a cosine distribution from the Knudsen cell with a unity sticking coefficient for Sc. As will be shown later, the Sc thickness deduced from the observed attenuation of the SiC substrate Si 2p and C 1s core levels in XPS was found to be in reasonable agreement with the calculated thickness/deposition rate.

The off axis (4° toward $(11\bar{2}0)$), 6H-SiC (0001) substrates utilized in this study were n-type ($N_d \approx 10^{18}$ cm^{-3}) and provided with a 1 μm, n-type ($N_d \approx 10^{17}$ cm^{-3}) 3C-SiC (111) epitaxial layer by Cree Inc. The unpolished sides of these wafers were coated with an opaque tungsten film via RF sputtering to increase the thermal heating efficiency of the SiC substrate, as the latter is transparent to the infra-red radiation emitted by the tungsten filament heater [18]. After sputter coating, the wafers were ultrasonicated in trichloroethylene, acetone, and methanol for 10 min each, and then dipped in 10:1 buffered HF for 10 min to remove the 100 nm thermal oxide previously grown on the SiC surface [19, 20]. The wafers were then subsequently annealed at 1050 °C in ~3×10^{-5} Torr SiH_4 in the GSMBE system for 15 min to desorb the remaining monolayer of surface oxide and produce a Si rich surface in XPS that exhibited a hexagonal (3×3) low energy electron diffraction (LEED) pattern [21, 22]. The SiC substrate was then annealed in 10^{-9} Torr vacuum to desorb the excess Si and produce an oxygen free, stoichiometric surface that displayed a hexagonal (1×1) LEED pattern [21, 22].

The GSMBE was connected to an ultrahigh vacuum transfer line that allowed for *in-situ* LEED, XPS, and UPS analysis of the Sc films [23]. The XPS and UPS measurements have been described previously and were performed in a separate vacuum chamber attached to the main UHV transfer line [24]. Briefly, all XPS spectra were collected using Al Kα radiation ($h\nu = 1484.6$ eV) in a 2×10^{-10} Torr UHV system equipped with a 100 mm diameter hemispherical electron energy analyser (VG CLAMII). The lens of the electron energy analyser was oriented at near normal incidence relative to the plane of the sample. Calibration of the binding energy scale for all scans was achieved by periodically taking scans of the Au $4f_{7/2}$ and Cu $2p_{3/2}$ peaks from standards and correcting for any discrepancies with the known values (83.98 and 932.67 eV, respectively). A combined Gaussian–Lorentzian curve shape with a linear background was found to best represent the data. UPS measurements were performed with the same energy analyser and a differentially pumped helium resonance UV lamp. The LEED optics was mounted on a six-way cross connected to the transfer line and pumped through the transfer line.

The method of Grant and Waldrop [25], previously described in detail [26], was utilized to determine the Schottky barrier (Φ_B) at the Sc/3C-SiC (111) interface. The method relies on referencing core levels (CLs) in the substrate to the valence band maximum (VBM) and then measuring how the position of those core levels change with the addition of the metal, as per:

$$\Phi_B(\mathrm{Sc/SiC}) = E_g - (E_{CL})_{int} + (E_{CL} - \mathrm{VBM})_{Bulk} \tag{1}$$

where E_g is the band-gap of the semiconductor (=2.4 eV for 3C–SiC [25]), $(E_{CL})_{int}$ is the substrate core level energy at the metal/semiconductor interface (relative to the Fermi level), and $(E_{CL} - \mathrm{VBM})$ is the relative position of the substrate core level to the VBM. To determine ΔCL_{int}, we performed successive depositions of 0.3–1 nm of Sc on the SiC surface and after each deposition measured the change in position of the Si 2p and C 1s in conjunction with the Sc $2p_{3/2,1/2}$ and other core levels. For $(E_{CL} - \mathrm{VBM})_{Bulk}$, we have previously determined the value of 99.3 ± 0.1 eV for the relative position of the Si 2p core level to the VBM for 3C–SiC (111) surfaces [16, 24].

3 Results and discussion Initial room temperature test depositions of Sc on the 3C-SiC (111)-(1x1) surface did not show a LEED pattern. As Kaplan has previously shown that Sc grows epitaxially on GaN (0001) surfaces at temperatures of 640–780 °C [1], growth of Sc on the 3C-SiC (111)-(1x1) surface was, therefore, investigated at a substrate temperature of 600 °C. Figure 1 shows XPS spectra of the Sc $2p_{3/2,1/2}$ core levels collected for a series of 0.3–1 nm thick layers of Sc consecutively evaporated onto the SiC surface. Prior to any Sc deposition, one can note a small peak in Fig. 1a at 398.4 eV that is attributed to the N 1s core level arising from the reaction of background NH_3 in the GSMBE with the 3C-SiC (111)-(1x1) surface during cleaning. The N 1s core level diminishes in intensity and eventually disappears as the cumulative deposited Sc thickness increases. The presence of the surface nitrogen in this study is believed to not induce additional band bending at the SiC surface or influence the Sc/SiC Schottky barrier measurements. Specifically, the presence of nitrogen in this study

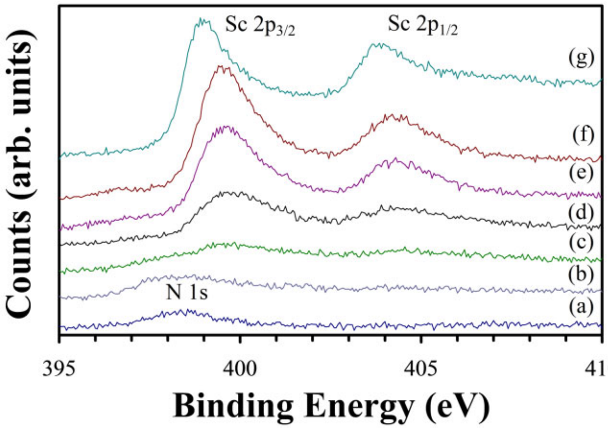

Figure 1 XPS of the Sc $2p_{3/2,1/2}$ and N 1s core levels from (a) 0 nm, (b) 0.3 nm, (c) 0.6 nm, (d) 0.9, (e) 2.2, (f) 3.2, and (g) >50 nm of Sc evaporated on a 3C–SiC (111)-(1x1) surface at 600 °C.

was not found to induce additional band bending relative to that of a prior investigation by the authors of SiC band bending where nitrogen was not observed [18].

For an approximately 3 nm thick Sc film (Fig. 1(f)), the Sc $2p_{3/2}$ was located at 399.6 ± 0.03 eV. This is slightly higher than the reported metallic value of 398.6 ± 0.2 eV [27], but substantially less than the values of 400.7 and 403.4 reported for ScN and Sc_2O_3, respectively [14, 27]. For a thick (~50 nm) Sc film evaporated onto the 3C-SiC surface, the Sc $2p_{3/2}$ was located closer to the metallic value at 399.0 eV (see Fig. 1(g)). The higher value for the Sc $2p_{3/2}$ could, therefore, be due to some upward band bending at the Sc/3C-SiC interface or reaction of Sc with the 3C-SiC surface to form $ScSi_x$ and/or ScC_x. Both of these possibilities will be discussed more later.

Figures 2 and 3 show XPS spectra of the F 1s and O 1s core levels for the same series of Sc depositions performed on the 3C-SiC (111)-(1x1) surface. As shown, the 3C-SiC (111)-(1x1) surface is free of F and O prior to any Sc deposition. However, some F and O contamination was observed after each Sc deposition and the intensity of the F 1s and O 1s increased with increasing Sc thickness. As mentioned previously, the F is attributed to the Sc charge and the refining process [14, 17]. The O is attributed to the reaction of Sc with background H_2O and O_2 in the GSMBE, XPS, and UHV transfer line. The total amount of F and O contaminants are estimated to be <5 at%.

Figures 4 and 5, respectively, show XPS spectra of the Si 2p and C 1s core levels from the 3C-SiC (111) substrate as a function of overlying Sc thickness. As expected, the intensity of these two peaks diminished with increasing Sc thickness. Assuming two-dimensional (2D)/Frank–van der Merwe growth (FM) [15], the attenuation of the Si 2p core level with increasing Sc thickness was found to be consistent with the calculated thickness based on the previously mentioned estimated Sc deposition rate. It has been previously shown that for 2D/FM growth, the

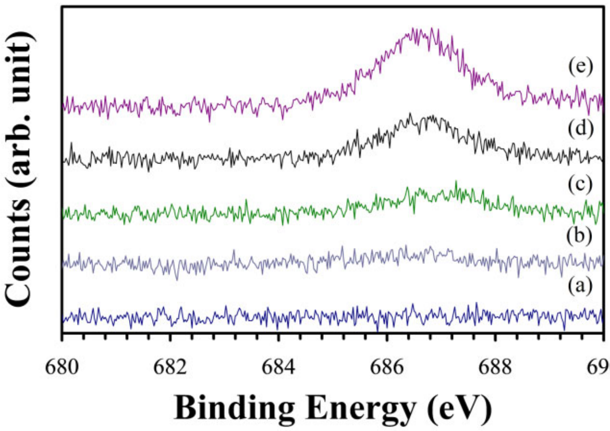

Figure 2 XPS of the F 1s core level from (a) 0 nm, (b) 0.3 nm, (c) 0.6 nm, (d) 0.9, and (e) 2.2 nm of Sc evaporated on a 3C-SiC (111)-(1x1) surface at 600 °C.

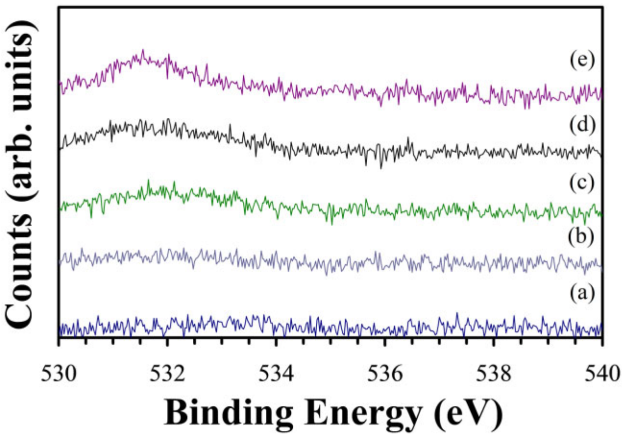

Figure 3 XPS of the O 1s core level from (a) 0 nm, (b) 0.3 nm, (c) 0.6 nm, (d) 0.9, and (e) 2.2 nm of Sc evaporated on a 3C-SiC (111)-(1x1) surface at 600 °C.

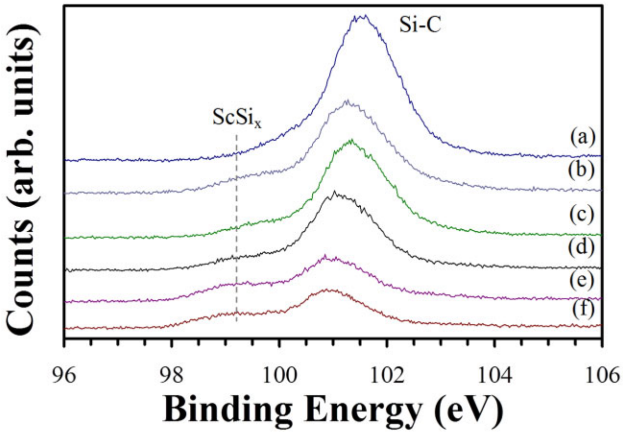

Figure 4 XPS of the Si 2p core level from (a) 0 nm, (b) 0.3 nm, (c) 0.6 nm, (d) 0.9, (e) 2.2 nm, and (f) 3.2 nm of Sc evaporated on a 3C-SiC (111)-(1x1) surface at 600 °C.

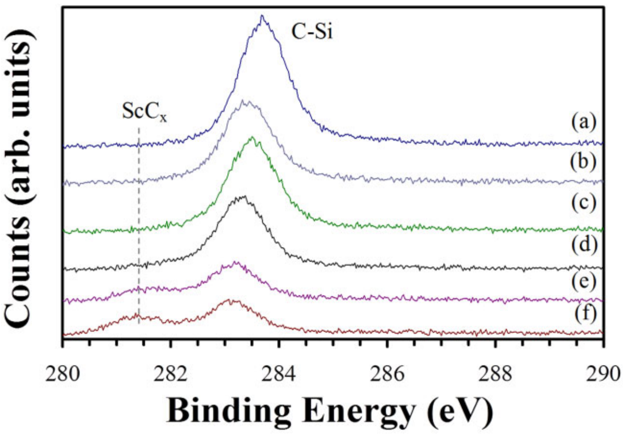

Figure 5 XPS of the C 1s core level from (a) 0 nm, (b) 0.3 nm, (c) 0.6 nm, (d) 0.9, (e) 2.2 nm, and (f) 3.2 nm of Sc evaporated on a 3C-SiC (111)-(1x1) surface at 600 °C.

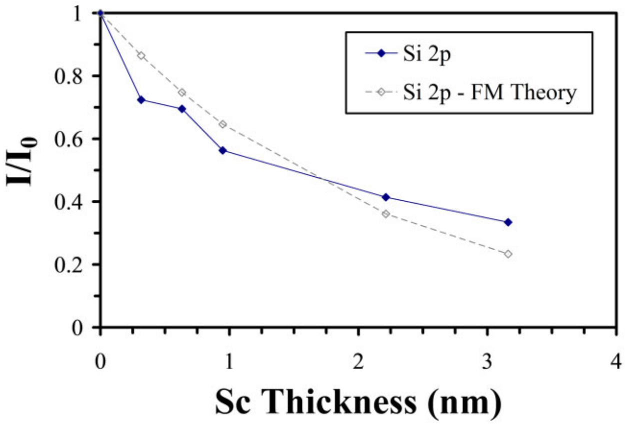

Figure 6 I/I_0 for 3C-SiC (111) Si 2p core level as a function of Sc film thickness.

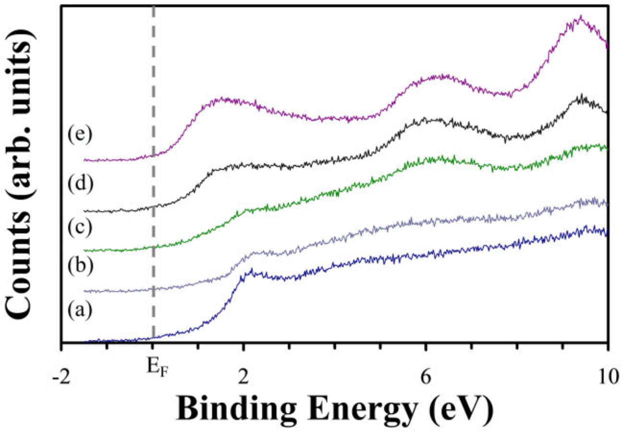

Figure 7 UPS spectra from (a) 0 nm, (b) 0.3 nm, (c) 0.6 nm, (d) 0.9, and (e) 2.2 nm of Sc evaporated on a 3C-SiC (111)-(1x1) surface at 600 °C.

attenuation of the substrate core level should follow the relation:

$$I/I_0 = \exp(-t/\lambda) \qquad (2)$$

where I_0 is the intensity of the uncoated substrate core level, I is the intensity of the substrate core level as a function of the film thickness (t), and λ is the inelastic mean free path of the substrate core level in the overlying film [15, 28]. The value of λ was determined to be 2.2 nm using previously described analytical expressions [15]. As shown in Fig. 6, the agreement between the observed attenuation (I/I_0) of the Si 2p core level with Sc thickness is in excellent agreement with the predicted attenuation based on FM theory. This is a strong indication that the growth of Sc on the 3C-SiC (111)-(1x1) surface occurred in a two-dimensional manner and that a continuous film was formed.

The Si 2p and C 1s core levels were also both observed to decrease in binding energy with increasing Sc thickness by ~0.5 eV for Sc thicknesses of 2–3 nm. This is indicative of upward band bending induced by the Sc deposition [18]. Similar band bending of ~0.4 eV has also been previously observed using XPS by Porter for room temperature deposition of Ti onto thermally cleaned 6H–SiC (0001)–(1x1) surfaces [28]. To further investigate the band bending, the UPS spectra shown in Fig. 7 were collected in tandem with XPS. For the clean and uncoated 3C-SiC (111)-(1x1) surface (Fig. 7(a)), UPS shows photoemission from surface states all the way up to the Fermi level (E_F). Surface states in the band gap of SiC of this nature have been previously observed in several photoemission studies of 6H-SiC (0001) surfaces [29–33]. These studies combined with our prior studies of hydrogen desorption from (0001)/(111) SiC surfaces [18] have shown that these surface states are attributable to surface Si-Si bonds arising due to the presence of Si adatoms on the (0001)/(111) SiC surface. The presence of these surface states, unfortunately, complicates locating the VBM in the clean 3C-SiC (111)-(1x1) spectra. The addition of Sc to the SiC surface (Fig. 7(b)–(e)) does not further clarify the situation with only Sc related states at ~6.3 and 9.4 eV gradually increasing in intensity with increasing Sc thickness.

In addition to the change in binding energy, additional peaks in the Si 2p and C 1s spectra were observed to appear at the higher Sc thicknesses. As shown in Fig. 4, a second peak (centered at 99.1 eV) appeared on the lower binding energy side of the main Si 2p core level at 101 eV. Similarly as shown in Fig. 5, a second peak centered at 281.4 eV also appeared on the lower binding energy side of the main C 1s core level at 283.2 eV. The higher binding energy Si 2p and C 1s core levels are both attributed to the Si–C bonding in the SiC substrate. The lower binding energy Si 2p peak is attributed to the formation of a $ScSi_x$ interfacial layer due to reaction of Sc with the SiC substrate [34]. The lower binding energy C 1s peak may likewise be evidence of interfacial ScC_x formation [35], although Sc_3C_4 is known to not be thermodynamically stable [35, 36] and in separate studies the authors were unsuccessful in growing Sc_3C_4 via GSMBE using evaporated Sc and ethylene gas. However, similar behaviour has been observed previously by Porter [28] and Grant and Waldrop [37–39] for Ti/6H-SiC (0001) interfaces where Ti was found to react with SiC to form a $TiSi_x$ and TiC interfacial layer.

The above XPS results correlate with the LEED measurements performed after each Sc deposition where a (2 × 2) LEED pattern was observed initially after the first 0.3 nm of Sc deposition. With additional Sc deposition, the LEED pattern returned to a (1 × 1) structure at 1 nm of Sc, and eventually after 3 nm of Sc deposition, no LEED pattern was observable. This indicates that the $ScSi_x/ScC_x$ interfacial layer formed between Sc and SiC is likely amorphous and is in contrast to Sc deposition on GaN (0001) surfaces at 640–780 °C where epitaxial growth of >20 nm thick Sc was observed to occur by Kaplan [1]. These contrasting results are likely a result of the different interfacial layers formed between the substrate and Sc. For the Sc/GaN interface, a ScN interfacial layer formed that, due to close lattice matching between ScN (111) and GaN (0001), was able to maintain an epitaxial relationship [1]. Due to the volatility of nitrogen, any free nitrogen created by the reaction of Sc with GaN was also able to leave the interface and escape into vacuum. However, for the Sc/SiC interface, an epitaxial relationship does not likely exist between $ScSi_x$, ScC_x, and SiC, and any free carbon or silicon formed by the interfacial reaction between Sc and SiC is trapped at the interface. Our results for Sc/3C-SiC (111) are closer to those by Porter where epitaxial growth of Ti on 6H–SiC (0001) surfaces was observed at room temperature, but annealing at 700 °C resulted in the formation of a complex reaction zone consisting of 2–3 nm TiC (111) in contact with SiC and overlaid by 10–15 nm of Ti_5Si_3 (0001) and Ti (0001) with imbedded TiC particles.

Using the value of 101.0 eV for the Si 2p core level observed for 2–3 nm thick Sc/3C-SiC (111) interfaces, the Schottky barrier was calculated using Eq. (1) and taking the band gap of 3C-SiC to be 2.4 eV and $(E_{\mathrm{Si2p}} - \mathrm{VBM})_{\mathrm{Bulk}} = 99.3 \pm 0.1$ eV as previously determined [24]. The Schottky barrier resulting from this calculation was determined to be 0.7 ± 0.1 eV. A value for the Schottky barrier can also be determined using the value of 283.1 eV for the C 1s from the same 2–3 nm Sc/3C-SiC (111) interfaces and the value of 281.3 ± 0.1 eV for $(E_{\mathrm{C1s}} - \mathrm{VBM})_{\mathrm{Bulk}}$ previously determined by Porter and Waldrop for 6H–SiC (0001) surfaces [25, 28]. Using these values, a slightly lower Schottky barrier of 0.6 ± 0.1 eV was determined. Taking the mean of these two values and using a root mean square average from the calculus of variations to combine the errors of the different measurements, we determine the Schottky barrier for the Sc/3C-SiC interface to be 0.65 ± 0.15 eV (see Fig. 8).

The Schottky barrier value for the Sc/SiC (111) interface is close to the value of 0.79 eV obtained by Porter based on XPS measurements of a Ti/6H–SiC (0001) interface formed at room temperature [28]. By similar methods, Waldrop and Grant obtained a slightly higher value of 0.97 eV for the Ti/6H–SiC (0001) Schottky barrier when the interface was annealed at 400 °C [38]. However for a Ti/3C-SiC (100) interface prepared at room temperature, Waldrop and Grant observed a smaller Schottky barrier of 0.53 eV [37]. These values bracket our results for the Sc/3C-SiC (111) interface and suggest that similar variability should be expected based on differences in SiC surface preparation and interface formation. The results also suggest that Sc should serve as an adequate Schottky/rectifying contact in SiC based devices.

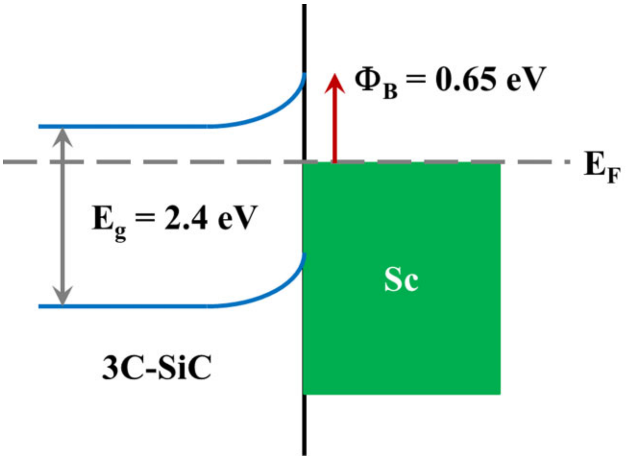

Figure 8 Schematic band diagram illustrating the magnitude of the Schottky barrier at the Sc/3C–SiC (111) interface.

4 Conclusions

XPS, UPS, and LEED have been utilized to investigate the interface formation and resulting Schottky barrier at interfaces formed by evaporation of Sc onto 3C-SiC (111)-(1x1) surfaces at 600 °C. Sc is observed to grow in a 2D manner with the first few nanometers exhibiting (1 × 1) LEED patterns suggestive of epitaxial growth. Continued growth results in the clear formation of a $ScSi_x$ and ScC_x interfacial layer and the loss of a LEED pattern. The Schottky barrier for the formed Sc/3C-SiC (111) interface was determined by XPS to be 0.65 ± 0.15 eV.

Acknowledgements The authors would like to thank Cree Inc. for supplying the 6H–SiC substrates. This work was supported by the ONR under contracts N00014-91-J-1410 and N00014-92-J1477, and by the Department of Education through an Electronic Materials Fellowship.

References

[1] R. Kaplan, S. Prokes, S. Binari, and G. Kelner, Appl. Phys. Lett. **68**, 3248 (1996).
[2] Z. Ahmad, JOM **55**, 35 (2003).
[3] M. Moram, M. Kappers, Z. Barber, and C. Humphreys, J. Cryst. Growth **298**, 268 (2007).
[4] M. Moram, Y. Zhang, M. Kappers, Z. Barber, and C. Humphreys, Appl. Phys. Lett. **91**, 152101 (2007).
[5] M. Akiyama, K. Umeda, A. Honda, and T. Nagase, Appl. Phys. Lett. **102**, 021915 (2013).
[6] R. Deng, K. Jiang, and D. Gall, J. Appl. Phys. **115**, 013506 (2014).
[7] M. Suzuki, T. Yanagitani, and H. Odagawa, Appl. Phys. Lett. **104**, 172905 (2014).
[8] S. Kerdsongpanya, B. Alling, and P. Eklund, J. Appl. Phys. **114**, 073512 (2013).
[9] S. Zhang, D. Holec, W. Fu, C. Humphreys, and M. Moram, J. Appl. Phys. **114**, 133510 (2013).
[10] S. Knoll, S. Rhode, S. Zhang, T. Joyce, and M. Moram, Appl. Phys. Lett. **104**, 101906 (2014).
[11] C. Constantin, H. Al-Brithen, M. Haider, D. Ingram, and A. Smith, Phys. Rev. B **70**, 193309 (2004).
[12] M. Little and M. Kordesch, Appl. Phys. Lett. **78**, 2891 (2001).
[13] L. Porter and R. Davis, Mater. Sci. Eng. B **34**, 83 (1995).
[14] S. King, R. Davis, and R. Nemanich, J. Vac. Sci. Technol. A **32**, 061504 (2014).
[15] S. King, E. Carlson, R. Therrien, J. Christman, R. Nemanich, and R. Davis, J. Appl. Phys. **86**, 5584 (1999).

[16] S. King, R. Davis, C. Ronning, M. Benjamin, and R. Nemanich, J. Appl. Phys. **86**, 4483 (1999).

[17] S. Kerdsongpanya, N. Nong, N. Pryds, A. Zakauskaite, J. Jensen, J. Birch, J. Lu, L. Hultman, G. Wingqvist, and P. Eklund, Appl. Phys. Lett. **99**, 232113 (2011).

[18] S. King, R. Davis, and R. Nemanich, Surf. Sci. **603**, 3104 (2009).

[19] S. King, R. Nemanich, and R. Davis, J. Electrochem. Soc. **146**, 1910. (1999).

[20] S. King, R. Nemanich, and R. Davis, J. Electrochem. Soc. **146**, 2648 (1999).

[21] S. King, R. Nemanich, and R. Davis, J. Electrochem. Soc. **146**, 3448 (1999).

[22] S. King, C. Ronning, R. Davis, R. Busby, and R. Nemanich, J. Appl. Phys. **84**, 6042 (1998).

[23] S. King, L. Smith, J. Barnak, J. Ku, J. Christman, M. Benjamin, M. Bremser, R. Nemanich, and R. Davis, MRS Proc. **395**, 739 (1996).

[24] S. King, R. Davis, C. Ronning, and R. Nemanich, J. Electron. Mater. **28**, L34 (1999).

[25] J. Waldrop, R. Grant, Y. Wang, and R. Davis, J. Appl. Phys. **72**, 4757 (1992).

[26] S. King, M. French, M. Jaehnig, M. Kuhn, B. Boyanov, and B. French, J. Vac. Sci. Technol. B **29**, 051207 (2011).

[27] J. Gimzewski, D. Fabian, L. Watson, and S. Affrossman, J. Phys. F **7**, L305 (1977).

[28] L. Porter, R. Davis, J. Bow, M. Kim, R. Carpenter, and R. Glass, J. Mater. Res. **10**, 668 (1995).

[29] J. Furthmuller, F. Bechstedt, H. Husken, B. Schroter, and W. Richter, Phys. Rev. B **58**, 13712 (1998).

[30] L. Johansson, L. Duda, M. Laurenzis, M. Krieftewirth, and B. Reihl, Surf. Sci. **445**, 109 (2000).

[31] C. Benesch, M. Fartmann, and H. Merz, Phys. Rev. B **64**, 205314 (2001).

[32] R. Ostendorf, K. Wulff, C. Benesch, and H. Zacharias, Surf. Sci. **600**, 3839 (2006).

[33] K. Emtsev, Th. Seyller, L. Ley, A. Tadich, L. Broekman, J. Riley, R. Leckey, and M. Preuss, Surf. Sci. **600**, 3845 (2006).

[34] V. Nemoshkalenko, A. Zakharov, V. Aleshin, and Y. Matveev, Theor. Exp. Chem. **13**, 529 (1978).

[35] R. Pottgen and W. Jeitschko, Inorg. Chem. **30**, 427 (1991).

[36] HSC Chemistry Software. (http://www.outotec.com/en/Products--services/HSC-Chemistry/). Outotec Oyi, P.O. Box 86, 02201 Espoo, Finland.

[37] J. Waldrop and R. Grant, Appl. Phys. Lett. **62**, 2685 (1993).

[38] J. Waldrop, J. Appl. Phys. **75**, 4548 (1994).

[39] J. Waldrop and R. Grant, Appl. Phys. Lett. **56**, 557 (1990).